

Scalar and Spinor Quasi Normal Modes of a 2D Dilatonic Blackhole

Pabitra Gayen* and Ratna Koley†

*Department of Physics, Presidency University,
86/1 College Street, Kolkata 700073, India.*

Abstract

External non-minimally coupled scalar and spinor field perturbations have been studied in a $(1 + 1)$ dimensional dilatonic blackhole spacetime [1, 2]. Exact analytical expressions of the quasi-normal mode frequencies have been found for both the cases. In the scalar perturbations the quasi-normal mode frequencies turn out to be purely imaginary and negative. Furthermore we have found that the quasi-normal frequencies for Dirac field exhibit both real and imaginary part. The QNM frequencies decay monotonically with the overtone number under certain class of the blackhole parameters. The decay profile ensures the stability of the blackhole spacetime under these perturbations.

* pabitra.rs@presiuniv.ac.in

† ratna.physics@presiuniv.ac.in

I. INTRODUCTION

Isolated black holes are just theoretical artifacts. In general, the blackholes are likely to be surrounded by perturbing scalar, vector, spinor and similar fields. The perturbed blackhole spacetimes are intrinsically dissipative due to the presence of the event horizon and the eigen modes of these systems are known as quasi-normal modes (QNMs). These modes possess a set of well defined complex frequencies known as quasi-normal frequencies (QNFs) [3]. We are particularly interested in studying the QNMs as they provide the window for an asymptotic observer to know the microscopic behaviour of blackholes (BHs). In recent times the QNMs are being widely studied in the context of gravitational wave astronomy as they are capable of giving precise information about the parameters of the blackhole as well as they can serve as a new tool to test the theories of gravity [4]. The QNM research has been expanded to encompass diverse topics like analogue gravity, alternative theories of gravity, higher dimensional spacetime etc [5–9]. Recent studies [10–14] also suggest that some of the major outstanding puzzles of modern cosmology - dark energy, dark matter or modified Newtonian dynamics at galactic scales, information loss beyond the blackhole horizon can be addressed by assuming the underlying microscopic quantum theory of gravity executing a multi-scale behaviour [15].

The work of Hawking and Penrose in the 1960s [16] showed the classical theory of gravity, GR, breaks down at certain regimes like the singularities at the cosmological big bang or gravitational collapse into black holes. The presence of singularities and event horizons, also leads to paradoxical situations such as information loss [17]. It is hoped that such paradoxes of the classical theory can be cured by quantizing gravity, which needs introduction of higher dimension. Such theories met with moderate success. On the other hand, GR being a non-linear theory and because of its inherent complexity, in four dimensions the exact analytical solutions are not easy to obtain. Classical GR becomes very much simpler in spacetime dimensions less than four, and this simplification carries over to the quantum theory as well. Although the lower dimensional models are not physical in the true sense of the term, the mathematical techniques and general reasoning are much the same as those for the full four-dimensional theory. In many situations, the understanding of a lower dimensional theory does provide important insights into the features of the actual four dimensional theory – for example, they have been proved to be very useful for investigating the blackhole

thermodynamics [18–21]. Many problems associated to full four dimensional theory can be addressed with much more control in lower dimensional toy models.

In this article we choose to work with a 2D line element that arises in the context of a stringy black hole proposed by Mandal-Sengupta-Wadia (MSW) [1] and also by Witten [2]. Without going into the details of how this line element is obtained we explore some intriguing features treating the geometry is given to us. However, interested reader may refer to the original references [1, 2] for necessary rigor. The geodesics and geodesic deviations in this geometry have been extensively studied in [22]. Several other aspects of classical and quantum gravity in MSW black hole spacetime in $(2+1)$ dimensions have been explored in [23–27] which include QNMs for minimally coupled massless and massive scalar field, Dirac field by using WKB approximation. In summary, the two dimensional blackhole spacetimes work as a great pedagogical tool. The two dimensional JT dilatonic black holes are quite well explored in the context of QNMs of non-minimally coupled perturbing scalar fields [15, 19, 28]. In the present work we picked up MSW [1] and tried to understand the basic features of the perturbations of a single horizon blackhole in 2D dilatonic gravity corresponding to the scalar and spin half fields. We studied perturbations due to *non-minimally coupled* massless and massive scalar fields with the dilatonic field. It is important to note that the coupling parameter plays an important role in the nature of QNFs and the stability of the blackhole geometry. It is crucial to note that exact analytical expressions for the QNM frequencies have been achieved in all the cases. Non-minimally coupled massless spin-half perturbations leads to QNFs which have both real and imaginary parts.

II. QUASI-NORMAL MODES FOR MASSIVE SCALAR PERTURBATIONS

It is well known that Einstein’s gravity is purely topological in two spacetime dimensions since the Einstein-Hilbert action is just the Gauss-Bonnet topological term. The presence of further structures like the dilaton field can invoke the dynamics. We choose to work with the first stringy black hole discovered in the early 1990s by Mandal et al. [1] and simultaneously by Witten [2] which arises in a low-energy effective description of dilatonic black holes in string theory:

$$S = \int d^2x \sqrt{-g} e^{-2\phi} [R + 4(\nabla\phi)^2 + 4\Lambda^2] \quad (1)$$

where ϕ is the dilaton field and Λ^2 is the cosmological constant. The spacetime is described by the following line element in the geometric unit with $G = 1$ and $c = 1$.

$$ds^2 = \left(1 - \frac{M}{r}\right) dt^2 - \frac{kdr^2}{4r^2 \left(1 - \frac{M}{r}\right)} \quad (2)$$

For the completeness, let us mention that M is connected to the mass of the black hole, k to the central charge parameter and ϕ to the dilaton field (with $e^\phi = \sqrt{\frac{M}{r}}$). As apparent from the metric, the horizon is at $r = M$ as $g_{tt} \rightarrow 0$ and $g_{rr} \rightarrow \infty$. The domain of our concern lies in the range $r > M$ in radial direction and $-\infty < t < \infty$ for time coordinate. Note that the spacetime is very similar to the $t-r$ section of the static, spherically symmetric Schwarzschild metric. The horizon is a point unlike a spherical surface in the case of a four dimensional blackhole. It is important to note that the above line element can be reduced to the familiar 2D dilatonic BH metric with a coordinate transformation $\bar{r} = \frac{\sqrt{k}}{2} \ln r$

$$ds^2 = -g(\bar{r})dt^2 + \frac{d\bar{r}^2}{g(\bar{r})} \quad (3)$$

where $g(\bar{r}) = 1 - M \exp(-2\Lambda\bar{r})$. Let us now give some other examples of black holes in two dimensional dilaton gravity. In the sense of full String Theory we note the exact metric

$$ds^2 = 2(k-2)[- \beta(r)dt^2 + dr^2] \quad (4)$$

where $\beta(r) = (\coth^2 r - 2/k)^{-1}$ as the dilaton is given as $\phi = \phi_0 + \frac{1}{2} \ln |\sinh^2 \frac{2r}{\beta}|$. For $k \rightarrow \infty$ limit the above metric reduces to the one obtained by Witten in [2]:

$$ds^2 = -\tanh^2 r dt^2 + dr^2 \quad (5)$$

This can also be obtained from the metric by Mandal *et.al.* [1] by a simple coordinate transformation. In this paper we choose to work with the line element given in Eq. (2).

Let us now consider an external scalar field Φ as the perturbing field. We have considered a generic coupling factor $h(\phi)$ between the dilaton and the perturbing field to ensure that the dynamics is properly captured in the Klein-Gordon equation [18]. For a massive scalar perturbation the Klein-Gordon equation in a general curved background is given by

$$\frac{1}{\sqrt{-g}h(\phi)} \partial_\mu (\sqrt{-g}h(\phi)g^{\mu\nu}\partial_\nu \Phi) + m^2\Phi = 0 \quad (6)$$

Since the metric coefficients - sourced by the background dilaton field - are function of r only, we can choose $h(\phi) = h(r)$ without loss of generality. Thus the time dependent part of the above equation will exhibit a harmonic nature. We now decompose $\Phi(r, t)$ in the following form

$$\Phi(r, t) = \frac{R(r)}{\sqrt{h(r)}} e^{-i\omega t} \quad (7)$$

to reduce the Eq. (6) in a form effectively analogous to a parametric harmonic oscillator, where ω is the frequency. The spatial wave function, $R(r)$, is defined in such a way that we achieve the simplest possible wave equation. Following the standard methodology let us introduce a generalized tortoise coordinate for the spacetime given in Eq. (2) as

$$r_* = \int \frac{dr}{\frac{2(r-M)}{\sqrt{k}}} = \frac{\sqrt{k}}{2} \ln \left(\frac{r-M}{\sqrt{k}} \right) \quad (8)$$

Note that, this transformation maps the horizon and the spatial infinity of radial coordinate into $r_* \rightarrow -\infty$ and $r_* \rightarrow \infty$ respectively. Under this coordinate transformation the radial part of Eq. (6) reduces to an equation analogous to the Schrodinger equation

$$\frac{d^2 R}{dr_*^2} + [\omega^2 - V_{eff}(r_*)] R = 0 \quad (9)$$

In radial coordinates the effective potential has the following form

$$V_{eff}(r) = \frac{2(r-M)}{kh(r)} \left((r-M) h''(r) + h'(r) - \frac{(r-M)}{2h} (h'(r))^2 \right) + \left(1 - \frac{M}{r} \right) m^2 \quad (10)$$

where prime denotes derivative w.r.t. r . The coupling term, $h(r)$ plays an important role in generating the modes of oscillation. It is apparent from the above expression that the massless modes are not supported without the coupling term. In fact, for a constant coupling the potential vanishes for massless case. A judicious choice of the function $h(r)$ leads to interesting features in the QNM spectrum. Implementing a power law behaviour, $h(r) \propto r^\sigma$, the potential in Eq. (10) reduces to the following form in tortoise coordinates

$$V_{eff}(r_*) = \frac{\sigma(\sigma-2)}{k} \xi^2 + \left(\frac{2\sigma}{k} + m^2 \right) \xi \quad (11)$$

where

$$\xi \equiv \frac{\sqrt{k}e^{2r_*/\sqrt{k}}}{M + \sqrt{k}e^{2r_*/\sqrt{k}}}. \quad (12)$$

The effective potential has been plotted in Figure 1 for the choice of parameters $\sigma = \frac{1}{2}$, $M = 1$, and $\sqrt{k} = 1$. In this figure we have shown the effective potentials experienced by fields having different masses. The figure depicts that effective potentials go to zero at the horizon and take different asymptotic values (depending on the mass of the fields) at spatial infinity. The nature of the potential may vary with the relative strengths of the blackhole parameters and the non-minimal coupling.

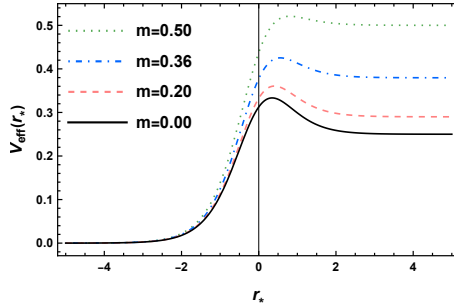


FIG. 1: Effective potential experienced by a massive scalar field in tortoise coordinates.

We now find the exact expressions for the QNM spectrum. They are characterised by the complex frequencies, the imaginary part of which causes damping of the modes. In general this can be obtained either by solving the Eq. (9) requiring the Dirichlet boundary conditions at infinity or by considering the modes are purely ingoing at the horizon [29]. At this point, we impose yet another transformation of coordinates to include the whole range ($-\infty < r_* < \infty$) of tortoise coordinate

$$x = \frac{1}{2} \left(1 + \tanh \frac{r_*}{\sqrt{k}} \right) \quad (13)$$

This change maps horizon to $x = 0$ and spatial infinity to $x = 1$. The functional form of the effective potential (11) in the new coordinates is given by

$$V_{eff}(x) = \frac{\sigma(\sigma - 2)x^2}{\left(M(1 - x) + \sqrt{k}x \right)^2} + \left(\frac{2\sigma}{k} + m^2 \right) \left(\frac{\sqrt{k}x}{M(1 - x) + \sqrt{k}x} \right) \quad (14)$$

We rewrite the Eq. (9) in the new coordinates to have the following form

$$\frac{4x^2(1 - x)^2}{k} \frac{d^2R}{dx^2} + \frac{4x(1 - x)(1 - 2x)}{k} \frac{dR}{dx} + (\omega^2 - V_{eff}(x)) R = 0 \quad (15)$$

According to the choice of the boundary condition, $R(x)$ is purely ingoing at the horizon and outgoing at spatial infinity. Let us construct $R(x)$ in the following way to achieve exact solutions of the above equation.

$$R(x) = x^\alpha (1-x)^\beta F(x) \quad (16)$$

with α and β satisfying

$$4\alpha^2 + k\omega^2 = 0 \quad km^2 + \sigma^2 - 4\beta^2 - k\omega^2 = 0 \quad (17)$$

where we have imposed a constraint $M = \sqrt{k}$ on the blackhole model parameters to achieve exact analytical results. The Eq. (15) reduces to a standard hypergeometric equation [30, 31] for $F(x)$ with the above construction (Eq. (16))

$$x(1-x) \frac{d^2F}{dx^2} + \left(\tilde{c} - \left(\tilde{a} + \tilde{b} + 1 \right) x \right) \frac{dF}{dx} - \tilde{a}\tilde{b}F = 0 \quad (18)$$

where

$$\tilde{a} = \alpha + \beta + 1 - \frac{\sigma}{2} \quad \tilde{b} = \alpha + \beta + \frac{\sigma}{2} \quad \tilde{c} = 2\alpha + 1. \quad (19)$$

We consider the following relations for the parameters α and β , to study Φ in detail

$$\alpha = i \frac{\omega\sqrt{k}}{2} \quad \beta = \frac{1}{2} \sqrt{km^2 + \sigma^2 - k\omega^2} \quad (20)$$

The solution of Eq. (18) is given by the standard hypergeometric function of second kind in Eq. (21) for \tilde{c} not being an integer

$$F(x) = C_1 {}_2F_1(\tilde{a}, \tilde{b}; \tilde{c}; x) + C_2 x^{1-\tilde{c}} {}_2F_1(\tilde{a} - \tilde{c} + 1, \tilde{b} - \tilde{c} + 1; 2 - \tilde{c}; x) \quad (21)$$

where C_1, C_2 are constants and ${}_2F_1$ is the hypergeometric function. We now impose the boundary conditions (i) purely ingoing near the horizon, (ii) purely outgoing for $x \rightarrow 1$ to calculate the QNMs. Purely ingoing behaviour of the solution near the horizon reduces $R(x)$ in the following form

$$R(x) = C_2 x^{-i\omega\sqrt{k}/2} (1-x)^{\sqrt{km^2 + \sigma^2 - k\omega^2}/2} {}_2F_1(\tilde{a} - \tilde{c} + 1, \tilde{b} - \tilde{c} + 1; 2 - \tilde{c}; x) \quad (22)$$

where we have set $C_1 = 0$ for the solution to be compatible with the boundary condition. The scalar quasinormal modes are purely outgoing at spatial infinity. We now use the Kummer's property [30, 31] of the hypergeometric function for further calculation

$$\begin{aligned}
{}_2F_1(\tilde{a}, \tilde{b}; \tilde{c}; x) &= \frac{\Gamma(\tilde{c})\Gamma(\tilde{c} - \tilde{a} - \tilde{b})}{\Gamma(\tilde{c} - \tilde{a})\Gamma(\tilde{c} - \tilde{b})} {}_2F_1(\tilde{a}, \tilde{b}; \tilde{a} + \tilde{b} + 1 - \tilde{c}; 1 - x) \\
&+ \frac{\Gamma(\tilde{c})\Gamma(\tilde{a} + \tilde{b} - \tilde{c})}{\Gamma(\tilde{a})\Gamma(\tilde{b})} (1 - x)^{\tilde{c} - \tilde{a} - \tilde{b}} {}_2F_1(\tilde{c} - \tilde{a}, \tilde{c} - \tilde{b}; \tilde{c} + 1 - \tilde{a} - \tilde{b}; 1 - x)
\end{aligned} \tag{23}$$

for \tilde{c} is not a negative integer [30] and $\tilde{c} - \tilde{a} - \tilde{b}$ is not an integer. In the limiting case when $r_* \rightarrow +\infty$ ($x \rightarrow 1$), imposing the above property of the hypergeometric function, $R(x)$ is reduced to

$$R \approx \frac{\Gamma(\tilde{C})\Gamma(\tilde{C} - \tilde{A} - \tilde{B})}{\Gamma(\tilde{C} - \tilde{A})\Gamma(\tilde{C} - \tilde{B})} e^{-\sqrt{km^2 + \sigma^2 - k\omega^2}r_*} + \frac{\Gamma(\tilde{C})\Gamma(\tilde{A} + \tilde{B} - \tilde{C})}{\Gamma(\tilde{A})\Gamma(\tilde{B})} e^{\sqrt{km^2 + \sigma^2 - k\omega^2}r_*} \tag{24}$$

where $\tilde{A} = \tilde{a} - \tilde{c} + 1$, $\tilde{B} = \tilde{b} - \tilde{c} + 1$, $\tilde{C} = 2 - \tilde{c}$. Applying the boundary condition that $F(x)$ is purely outgoing at the asymptotic limit is therefor equivalent to imposing the condition

$$\tilde{C} - \tilde{A} = -n \quad \text{or} \quad \tilde{C} - \tilde{B} = -n, \tag{25}$$

where $n = 0, 1, 2, \dots$ is the overtone number. We thus get the quasinormal frequencies (QNFs) for the massive scalar field Φ as

$$\omega' = -i \frac{(4n^2 + 4n\sigma - km^2)}{2\sqrt{k}(2n + \sigma)} \quad \omega'' = -i \frac{(4(n + 1)(n + 1 - \sigma) - km^2)}{2\sqrt{k}(2n + 2 - \sigma)} \tag{26}$$

We have shown the variation of the QNFs with overtone number in Figure 2 where we have considered the imaginary part of the QNF is negative. As is well known, for the stability of the modes in Eq. (7) the amplitude should decay with time at any fixed spatial position. The modes will lead to stability under the condition

$$n > \frac{1}{2} \left(\sqrt{km^2 + \sigma^2} - \sigma \right) \quad \text{for } n \geq 1 \tag{27}$$

It is worth noting that the frequency ω' will not give any stable mode for $n = 0$ whereas one can achieve stability for ω'' under the condition $2 > \sqrt{km^2 + \sigma^2} + \sigma$.

Time evolution of square of different massive scalar modes in logarithmic scale at $r = 10$ is shown in the Figure 3 and 4. It is seen that as the mass of the field increases the mode becomes less and less damped for a fixed value of n . It is also clear that the damping of a particular massive mode increases with the increase of n .

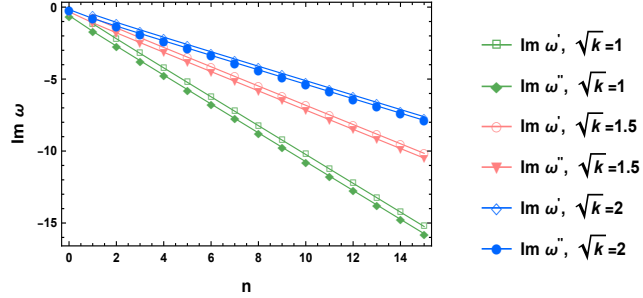


FIG. 2: Variation of imaginary part of QNFs for massive ($m = 0.5$) scalar field with n for different \sqrt{k} values. Considering the values of the parameters $M = 1$ and $\sigma = 0.5$.

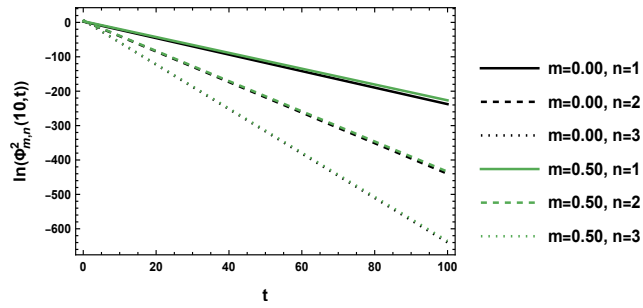


FIG. 3: Time evolution of square of different massive scalar modes in logarithmic scale at $r = 10$ corresponding to the frequency ω' . Considering the value of the parameter $\sqrt{k} = 1$.

III. QUASI-NORMAL MODES FOR MASSLESS DIRAC FIELD NON-MINIMALLY COUPLED WITH DILATON FIELD

We propose a scalar-fermion Yukawa type, non-minimal coupling between the dilaton and the Dirac field in the background geometry of Eq. (2). The action for a massive Dirac field with this coupling is given by

$$S = \int d^2x \sqrt{-g} [\bar{\Psi} (i\gamma^\mu \nabla_\mu - m) \Psi - \zeta(r) \phi \bar{\Psi} \Psi] \quad (28)$$

The term, $\zeta(r)\phi$ can be written as m_{eff} in the following action in Eq. (29) by considering $m_{eff} = \zeta(r)\phi$. For further exploration we have chosen a power law behavior for m_{eff} as Qr^σ because the dilaton field is function of radial coordinate only. Thus we see from the above action that a massless Dirac field also picks up an effective mass parameter due to the interaction term and the above action reduces to the following form

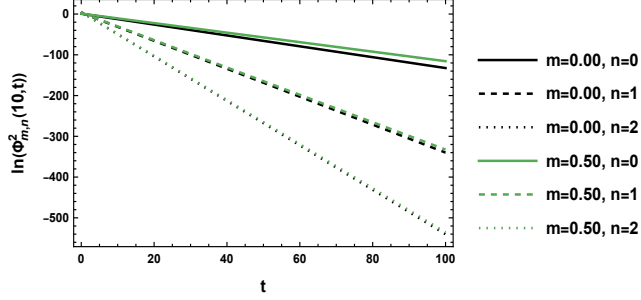


FIG. 4: Time evolution of square of different massive scalar modes in logarithmic scale at $r = 10$ corresponding to the frequency ω'' .

$$S = \int d^2x \sqrt{-g} \bar{\Psi} (i\gamma^\mu \nabla_\mu - m_{eff}) \Psi \quad (29)$$

Variation of the above action with respect to $\bar{\Psi}$ leads to the equation of motion of the Dirac field as

$$i\bar{\nabla}\Psi = m_{eff}\Psi \quad (30)$$

where Ψ is a two-spinor, $\bar{\nabla}$ ($= \gamma^\mu \nabla_\mu$) is Dirac slash operator with ∇_μ ($= \partial_\mu - \Gamma_\mu$) being the covariant derivative and Γ_μ is the spin connection. We write the metric in Eq. (2) in tortoise coordinate as given in Eq. (8) to work with the Dirac equation in MSW background

$$ds^2 = \xi d\tilde{s}^2 = \xi(dt^2 - dr_*^2) \quad (31)$$

where ξ is given in Eq. (12). Considering a conformal transformation, $g_{\mu\nu} = \xi \tilde{g}_{\mu\nu}$, of the metric in Eq. (2), the relevant quantities in Dirac equation reduce to the following form [32]

$$\Psi = \frac{1}{\xi^{1/4}} \tilde{\Psi}, \quad \bar{\nabla}\Psi = \frac{1}{\xi^{3/4}} \tilde{\nabla}\tilde{\Psi}, \quad m_{eff} = \frac{1}{\xi^{1/2}} \tilde{m} \quad (32)$$

The Dirac equation (30) reduces to a pair of coupled differential equations containing $\tilde{\Psi}_1$ and $\tilde{\Psi}_2$ which are components of the two dimensional Dirac spinor.

$$\begin{aligned} \partial_t \tilde{\Psi}_2 - \partial_{r_*} \tilde{\Psi}_2 &= -im_{eff} \sqrt{\xi} \tilde{\Psi}_1 \\ \partial_t \tilde{\Psi}_1 + \partial_{r_*} \tilde{\Psi}_1 &= -im_{eff} \sqrt{\xi} \tilde{\Psi}_2. \end{aligned} \quad (33)$$

Employing the same method as used for scalar perturbation we decompose the radial and temporal part of $\tilde{\Psi}$ as

$$\tilde{\Psi}_s(r_*, t) = R_s(r_*) e^{-i\omega t}, \quad s = 1, 2 \quad (34)$$

Note that the function ξ is dependent on r_* only. As a result the temporal part exhibits a harmonic oscillator nature. Redefinition of R_1 by $e^{i\pi/4}\tilde{R}_1$, and R_2 by $e^{-i\pi/4}\tilde{R}_2$ reduces the above set of equations (33) in the following form

$$\begin{aligned} \frac{d\tilde{R}_2}{dr_*} + i\omega\tilde{R}_2 &= -m_{eff}\sqrt{\xi}\tilde{R}_1 \\ \frac{d\tilde{R}_1}{dr_*} - i\omega\tilde{R}_1 &= -m_{eff}\sqrt{\xi}\tilde{R}_2 \end{aligned} \quad (35)$$

The QNM mode analysis is done by choosing linear combinations of \tilde{R}_1 and \tilde{R}_2 as $Z_{\pm} = \tilde{R}_1 \pm \tilde{R}_2$. They will in turn give us the left and right chiral modes. The equation for Z_{\pm} can be written in a Schrodinger like form in tortoise coordinate as

$$\frac{d^2Z_{\pm}}{dr_*^2} + \omega^2 Z_{\pm} = V_{\pm}(r_*)Z_{\pm} \quad (36)$$

Effective potentials for the spinor modes have the following form

$$V_{\pm}(r_*) = Q (W(r_*))^{\sigma-2} \left(\sqrt{k} Q e^{\frac{2r_*}{\sqrt{k}}} (W(r_*))^{\sigma+1} \mp \frac{\sqrt{e^{\frac{4r_*}{\sqrt{k}}}} \left(2\sqrt{k}\sigma e^{\frac{2r_*}{\sqrt{k}}} + M \right)}{\sqrt{1 - \frac{M}{W(r_*)}}} \right) \quad (37)$$

where $W(r_*) = \left(\sqrt{k} e^{\frac{2r_*}{\sqrt{k}}} + M \right)$. The effective potentials experienced by the modes for different values of constant Q associated with the coupling term are plotted in Fig. (5) and (6) with the choice of the parameters $\sigma = -\frac{1}{2}$, $M = 1$ and $\sqrt{k} = 1$. It is apparent from the figures that the effective potential will vanish at the horizon and at spatial infinity. The potentials also exhibit interesting features depending on different values Q .

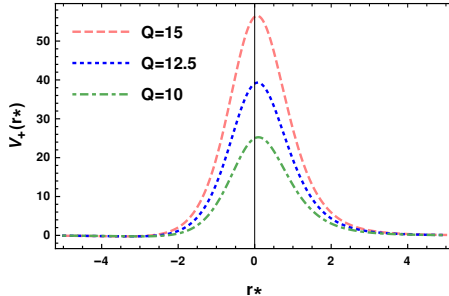


FIG. 5: Effective potential experienced by Z_+ mode for different Q in tortoise coordinates with parameters $\sigma = -\frac{1}{2}$, $M = 1$ and $\sqrt{k} = 1$.

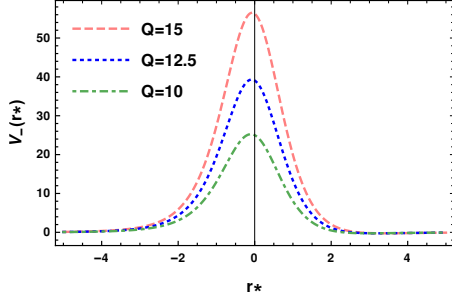


FIG. 6: Effective potential experienced by Z_- mode for different Q in tortoise coordinates with parameters $\sigma = -\frac{1}{2}$, $M = 1$ and $\sqrt{k} = 1$.

We now obtain decoupled equations for R_1 and R_2 from the coupled set of equations in Eq. (33)

$$\frac{1}{\xi} \frac{d^2 R_s}{dr_*^2} + \frac{m_{eff}}{\sqrt{\xi}} \frac{d}{dr_*} \left(\frac{1}{m_{eff} \sqrt{\xi}} \right) \frac{dR_s}{dr_*} + \frac{im_{eff}\omega\epsilon}{\sqrt{\xi}} \frac{d}{dr_*} \left(\frac{1}{m_{eff} \sqrt{\xi}} \right) R_s + \frac{\omega^2}{\xi} R_s = m_{eff}^2 R_s \quad (38)$$

where $\epsilon = \mp 1$ for $s = 1$ and 2 respectively. Considering the coordinate transformation given in Eq. (13) along with $\sqrt{k} = M$, $\sigma = -\frac{1}{2}$ and having α_s and β_s to satisfy the following relations

$$\alpha_s = \begin{cases} \frac{1}{2} (iM\omega\epsilon + 1) \\ -\frac{i}{2} M\omega\epsilon \end{cases} \quad \beta_s = \begin{cases} \frac{1}{2} (-iM\omega\epsilon + 1) \\ \frac{i}{2} M\omega\epsilon \end{cases} \quad (39)$$

one can reduce Eq. (38) to the standard hypergeometric differential equation form by substituting $R_s(x) = x^{\alpha_s} (1-x)^{\beta_s} F_s(x)$

$$x(1-x) \frac{d^2 F_s}{dx^2} + (c_s - (a_s + b_s + 1)x) \frac{dF_s}{dx} - a_s b_s F_s = 0 \quad (40)$$

where

$$a_s = \alpha_s + \beta_s - \frac{iQ\sqrt{M}}{2}, \quad b_s = \alpha_s + \beta_s + \frac{iQ\sqrt{M}}{2}, \quad c_s = 2\alpha_s + \frac{1}{2}. \quad (41)$$

For $\epsilon = 1$, the solution of Eq. (40) reveals the following form of R_2

$$R_2 = \tilde{C}_1 x^{(iM\omega+1)/2} (1-x)^{iM\omega/2} {}_2F_1(a_2, b_2; c_2; x) + \tilde{C}_2 x^{-iM\omega/2} (1-x)^{iM\omega/2} {}_2F_1(a_2 - c_2 + 1, b_2 - c_2 + 1; 2 - c_2; x). \quad (42)$$

We now apply the boundary condition that the modes are purely ingoing near the horizon. So we can choose $\tilde{C}_1 = 0$ to write R_2 in the following form

$$R_2 = \tilde{C}_2 x^{-iM\omega/2} (1-x)^{iM\omega/2} {}_2F_1(a_2 - c_2 + 1, b_2 - c_2 + 1; 2 - c_2; x) \quad (43)$$

In the limit of spatial infinity *i.e.* for $r_* \rightarrow +\infty$ ($x \rightarrow 1$) we get R_2 in the following form by applying Kummer's property of the hypergeometric functions given in Eq. (23).

$$R_2 \approx \frac{\Gamma(C_2)\Gamma(C_2 - A_2 - B_2)}{\Gamma(C_2 - A_2)\Gamma(C_2 - B_2)} e^{-i\omega r_*} + \frac{\Gamma(C_2)\Gamma(A_2 + B_2 - C_2)}{\Gamma(A_2)\Gamma(B_2)} e^{-\frac{r_*}{M} + i\omega r_*} \quad (44)$$

where $A_2 = a_2 - c_2 + 1$, $B_2 = b_2 - c_2 + 1$, $C_2 = 2 - c_2$. Imposing the condition that the modes are purely outgoing asymptotically, we obtain the following conditions

$$C_2 - A_2 = -n \quad \text{or} \quad C_2 - B_2 = -n, \quad \text{where } n = 0, 1, 2, \dots \quad (45)$$

The QNFs for the component Ψ_2 of the Dirac field turn out to be

$$\omega_I = \frac{Q}{2\sqrt{M}} - \frac{i}{M} \left(n + \frac{1}{2} \right) \quad \omega_{II} = -\frac{Q}{2\sqrt{M}} - \frac{i}{M} \left(n + \frac{1}{2} \right) \quad (46)$$

One can get the similar set of QNFs (46) for the component Ψ_1 of the Dirac field by applying the similar procedure. From these expressions of QNFs for both components Ψ_1 and Ψ_2 , it is clearly seen that QNFs have both real and imaginary parts. The real parts scale linearly with Q , constant associated with coupling and imaginary parts are independent of that. On the other hand negative imaginary parts scale linearly with the overtone number, n where as real parts are independent of n . QNFs up to overtone number 5 have been presented in Table I for different field couplings.

QNFs corresponding to Eq. (46) have both real and imaginary parts so the modes provide damped oscillatory behaviour during their temporal evolution at an observation position. Since the imaginary part of QNFs are independent of Q , the damping is also independent of the coupling strength. On the other hand, the real part scales linearly with the coupling constant so depending on the strength of coupling the oscillation frequency of the modes will change. These features of the modes can be clearly seen in the Figure (7) and (8) for Ψ_2 component of Dirac field. Time evolution of modulus of Ψ_2 at a given position for different values of Q is shown using a logarithmic scale. Figures depict that the damping of a mode

increases with increasing overtone number. Modes from larger Q value have larger oscillation frequency compared to other modes produced from lower Q values for same overtone number, n .

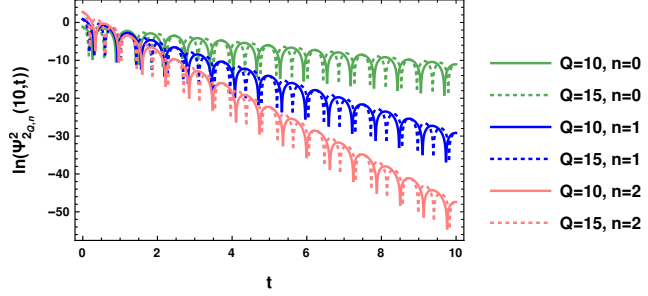


FIG. 7: In logarithmic scale the time evolution of square of Ψ_2 component of the Dirac field with different Q values at $r = 10$ corresponding to QNFs ω_I has been shown.

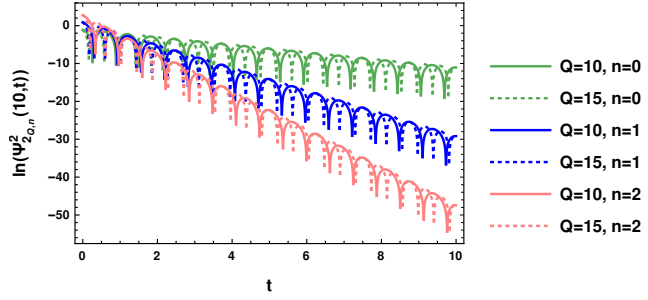


FIG. 8: Time evolution of square of Ψ_2 component of the Dirac field with different Q values at $r = 10$ corresponding to QNFs ω_{II} has been depicted in logarithmic scale. It is seen that as Q increases the mode becomes more and more oscillatory for a fixed value of n . It is also clear that the damping of a particular mode increases with the increase of n .

IV. CONCLUSIONS

Blackhole quasi normal modes are of particular interest as they depend only on intrinsic blackhole parameters. They can be useful in estimating the parameters of the blackhole. The other importance lies in the fact that QNMs can be used in the semi-classical attempts to quantize a black hole area. In this work there are two distinct results. The exact solutions of the quasi normal mode frequencies have been obtained for both Klein-Gordon and Dirac field. These can provide us with better understanding of the perturbation theory as they

TABLE I: Real and imaginary parts of QNFs for the components Ψ_1 and Ψ_2 of the Dirac field for different values of Q and n considering $M = 1$.

$Q = 10$				$Q = 15$		
n	$Re \omega_I$	$Re \omega_{II}$	$Im \omega_I$ or $Im \omega_{II}$	$Re \omega_I$	$Re \omega_{II}$	$Im \omega_I$ or $Im \omega_{II}$
0	5	-5	-0.5	7.5	-7.5	-0.5
1	5	-5	-1.5	7.5	-7.5	-1.5
2	5	-5	-2.5	7.5	-7.5	-2.5
3	5	-5	-3.5	7.5	-7.5	-3.5
4	5	-5	-4.5	7.5	-7.5	-4.5
5	5	-5	-5.5	7.5	-7.5	-5.5

d dictate the late time behaviour of the fields. In all the cases the modes scale with the black-hole parameters k and M . They also depend on the mass of the perturbing Klein-Gordon field in general , however, the dependence can be negligibly small for largely damped modes under certain restrictions on the parameters of the theory. For the Klein-Gordon field, we have chosen a non-minimal coupling of the dilaton field with the perturbing scalar to study the stability under scalar perturbations. It is worthy noting that the massless modes are supported by the non-minimal coupling term, *i.e.* in the absence of this there will no such quasi normal mode in the scalar case. The QNMs are stable against these types of perturbations but there are possibilities for the existence of unstable modes depending on the masses of the perturbing fields and the coupling of the fields with the dilaton (for scalar perturbations). Here we have chosen a power law dependence, however, it may be interesting to explore the consequences of other kinds of coupling functions. It has been found for Klein-Gordon field, in a particular stable mode the most massive field experiences the least damping compared to other fields. Damped oscillatory feature has been found in the time evolution profile of Dirac field and oscillation frequency increases with the of increase of coupling strength with the dilaton but damping is independent of it. For both types of fields, the damping feature increases with the increase of overtone number *i.e.* more the overtone number, a field is more damped.

We propose to explore how these exact expressions of the quasi-normal frequencies can be

used to find a relation between the highly damped modes and the quantum area of the black hole. As the QNFs are complex, in this case Maggiore's [33] proposal will be applicable. The QNM spectrum in the heavily damped limit will be treated as a harmonic oscillator with frequency $\omega = \sqrt{\omega_R^2 + \omega_I^2}$. In future we would like to explore how QNMs can be related to the blackhole intrinsic microscopic properties. We further like to explore how the blackhole can be understood as an ensemble of harmonic oscillators exploiting the large n limit of quasi normal modes.

V. ACKNOWLEDGEMENTS

P. Gayen acknowledges the University Grants Commission (UGC), India for providing financial support through a fellowship with ID: 191620137660.

- [1] G. Mandal, A. M. Sengupta, and S. R. Wadia, *Mod. Phys. Lett. A* **6**, 1685 (1991).
- [2] E. Witten, *Phys. Rev. D* **44**, 314 (1991).
- [3] K. D. Kokkotas and B. G. Schmidt, *Living Rev. Rel.* **2**, 2 (1999), arXiv:gr-qc/9909058.
- [4] K. G. Arun *et al.* (LISA), *Living Rev. Rel.* **25**, 4 (2022).
- [5] S. Chakraborty, K. Chakravarti, S. Bose, and S. SenGupta, *Phys. Rev. D* **97**, 104053 (2018).
- [6] P. Kanti and R. A. Konoplya, *Phys. Rev. D* **73**, 044002 (2006).
- [7] D. Birmingham, I. Sachs, and S. N. Solodukhin, *Phys. Rev. Lett.* **88**, 151301 (2002).
- [8] P. K. Kovtun and A. O. Starinets, *Phys. Rev. D* **72**, 086009 (2005).
- [9] S. S. Seahra, C. Clarkson, and R. Maartens, *Phys. Rev. Lett.* **94**, 121302 (2005).
- [10] E. P. Verlinde, *SciPost Phys.* **2**, 016 (2017).
- [11] M. Tuveri and M. Cadoni, *Phys. Rev. D* **100**, 024029 (2019).
- [12] G. Dvali, *JHEP* **03**, 126 (2021).
- [13] G. Dvali and C. Gomez, *JCAP* **01**, 023 (2014).
- [14] M. Cadoni, M. Tuveri, and A. P. Sanna, *Symmetry* **12**, 1396 (2020).
- [15] M. Cadoni, M. Oi, and A. P. Sanna, *JHEP* **01**, 087 (2022).
- [16] S. W. Hawking and G. F. R. Ellis, *The Large Scale Structure of Space-Time*, Cambridge Monographs on Mathematical Physics (Cambridge University Press, New York, 2023).

- [17] J. Preskill, in *International Symposium on Black holes, Membranes, Wormholes and Superstrings* (1992).
- [18] J. Kettner, G. Kunstatter, and A. J. M. Medved, *Class. Quant. Grav.* **21**, 5317 (2004), arXiv:gr-qc/0408042.
- [19] S. Bhattacharjee, S. Sarkar, and A. Bhattacharyya, *Phys. Rev. D* **103**, 024008 (2021), arXiv:2011.08179 [gr-qc].
- [20] D. Grumiller, W. Kummer, and D. V. Vassilevich, *Phys. Rept.* **369**, 327 (2002).
- [21] R. Mann, A. Shiekh, and L. Tarasov, *Nucl. Phys. B* **341**, 134 (1990).
- [22] R. Koley, S. Pal, and S. Kar, *Am. J. Phys.* **71**, 1037 (2003), arXiv:gr-qc/0302065.
- [23] S. Fernando, *Gen. Rel. Grav.* **37**, 461 (2005).
- [24] S. Fernando, *Gen. Rel. Grav.* **36**, 71 (2004).
- [25] K. C. K. Chan and R. B. Mann, *Phys. Rev. D* **50**, 6385 (1994).
- [26] S. Sebastian and V. C. Kuriakose, *Mod. Phys. Lett. A* **29**, 1450019 (2014).
- [27] A. Lopez-Ortega and I. Vega-Acevedo, *Gen. Rel. Grav.* **43**, 2631 (2011).
- [28] A. Zelnikov, *JHEP* **07**, 010 (2008).
- [29] B. F. Schutz and C. M. Will, *Astrophys. J. Lett.* **291**, L33 (1985).
- [30] M. Abramowitz, I. A. Stegun, *et al.*, *Handbook of mathematical functions* (Dover, New York, 1964).
- [31] Z. X. Wang and D. R. Guo, *Special functions* (World Scientific, Singapore, 1989).
- [32] A. Lopez-Ortega, *Lat. Am. J. Phys. Educ.* **3**, 578 (2009).
- [33] M. Maggiore, *Phys. Rev. Lett.* **100**, 141301 (2008), arXiv:0711.3145 [gr-qc].